TECHNICAL UNIVERSITY OF CLUJ-NAPOCA

ACTA TECHNICA NAPOCENSIS

Series: Applied Mathematics, Mechanics, and Engineering
Vol. 67, Issue Special I, February, 2024

SIMULATION BY FEM OF TIG DEPOSITION WELDING OF MULTICOMPONENT ALLOY ON CARBON STEEL SUBSTRATE

George SIMION, Dan BÎRSAN, Ionelia VOICULESCU, Elena SCUTELNICU

Abstract: *Due to the high cost of multicomponent alloys production, the applicability of these materials is still limited in industry. However, the deposition welding or cladding process should be taken into consideration as a less expensive method, more afforded for achieving these special materials that could be employed for many industrial applications. This paper presents a numerical model used to simulate the deposition welding of a multicomponent alloy from the AlCrFeNi system on S235 structural steel substrate. The model was experimentally validated by measuring the temperature and stress developed during the cladding process. The numerical results revealed the pick temperature around 1700-1800°C in the molten pool and the equivalent stress of 600-700MPa in the deposited material.*

Key words: *multicomponent alloy, cladding, numerical simulation, temperature, equivalent stress*

1. INTRODUCTION

In the last decades, a new concept of making metallic alloys, by combining at least four or five chemical elements in equiatomic or quasi-atomic proportions, with concentrations between 5% and 35%, has attracted the attention of researchers around the world [1–5]. In the scientific literature, the most frequently used name for this new category of materials is "High Entropy Alloys" (HEAs). However, some researchers consider that entropy is not the determining factor of these materials and, therefore, other names are proposed such as multicomponent alloys, compositionally complex alloys, or multi-element alloys [5]. In 2004, the first two articles on multicomponent alloys were published and, since then, their number has steadily increased. Due to the unique composition of high entropy alloys, they can develop outstanding mechanical characteristics, including high strength and hardness, outstanding resistance to wear, corrosion and oxidation at high temperatures, and good structural stability. Some of these properties exceed those of conventional alloys, making HEAs attractive in many industrial fields [6]. Some multicomponent alloys have remarkable mechanical characteristics [7–16]. For instance, $Al_{20}Li_{20}Mg_{10}Sc_{20}Ti_{30}$ has 5.9GPa hardness and 2.67g/cm^3 density, being three times lower than that of steel [17]; $AlCoCrFeMo_{0.3}Ni$ is characterized by 2.65GPa yield strength and 3.2GPa tensile strength [18]; $MoNbTiV_{0.75}Zr$ has 1.7GPa yield strength and 3.9GPa tensile strength [19], and $V_{10}Cr_{15}Mn_5Fe_{35}Co_{10}Ni_{25}$ alloy that has elongation of 700-770% at temperatures of 700-800°C [20]. The researchers reported that the main characteristic of multicomponent alloys is their ability to maintain the mechanical characteristics at low [21,22] or high temperatures [23,24], which recommends them to replace some traditional alloys used in industrial applications.

Because of the high production costs of multicomponent alloys, determined by the price of raw materials, expensive equipment used in fabrication, and the numerous technological preparations that are required for their obtaining, the applicability of this materials type is still limited in industry. For alternative solutions, researchers worldwide have investigated the possibility of deposition welding of these new alloys on ordinary materials, in order to improve the surface quality of traditional basic materials that can be achieved at much lower costs [25–

29]. Cladding of multicomponent alloys on common steels can be a suitable solution for improving the technology transfer from the research field to industry. In the scientific literature, several processes have been identified for the deposition of multicomponent alloys on the substrate material surface, usually common steel, such as magnetron sputtering [30,31], Laser cladding [32,33], TIG welding cladding [34,35], and sintering [36,37].

This work describes and discusses the effects of deposition welding of multicomponent material, belonging to the AlCrFeNi alloy system, on S235 steel substrate material. The high hardness and wear resistance [37–39] of the material achieved make it appropriate for industrial cladding applications.

The aim of this investigation was to develop a numerical model for estimating the temperature field and the strain and stress level in the material deposited by TIG welding. To the best of our knowledge, no numerical model developed for the prediction of thermal and mechanical effects determined by the TIG cladding process in multicomponent alloys has been reported so far.

2. MATERIALS AND METHODS

2.1. Materials

On an S235 steel plate, having 12 mm thickness, and the configuration and dimensions shown in Figure 1, several $AlCr_{0.7}FeNi$ weld beads were deposited by the TIG welding process. The chemical compositions and the mechanical characteristics of the base and filler materials are shown in Tables 1 and 2.

Table 1

Chemical composition of materials

Material	C [%]	Mn [%]	Si [%]	Cr [%]	Fe [%]	Ni [%]	Mo [%]	Nb [%]	Al [%]	Co [%]	Cu [%]	Ti [%]
S235	0,12	0,75	0,17	0,04	98,2	0,03	0,0,2	-	0,04	-	0,06	0,001
$AlCr_{0,7}FeNi$	0,01	0,64	0,25	19,3	26,7	31,5	5,16	1,59	14,6	0,01	0,05	0,08

Table 2

Mechanical characteristics of base and filler material

Material	Tensile strength σ_{uts} [MPa]	Elongation [%]	Hardness [HV]
S235	440-450	32	155-190
$AlCr_{0,7}FeNi$	1400-2100	0-40	500-800

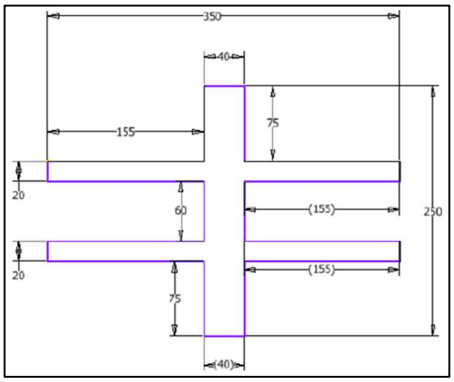

Fig. 1. Geometry and dimensions of S235 steel plate.

2.2. Experiments

Four weld beads of $AlCr_{0.7}FeNi$ multicomponent alloy were deposited on the S235 substrate by TIG welding, whose process parameters are shown in Table 3. In order to avoid the development of cracks, which is a frequent defect when dissimilar materials are welded [40,41], the interpass temperature between the multicomponent depositions was maintained at about 250-300°C. To measure temperatures in several positions, type K thermocouples and Lutron BTM-4208SD data acquisition device were used. Also, for stress measurement, strain gauges type 10/120 LY11 and QuantumX device were employed and the CatmanEASY software program was used to process the data recorded during the process.

Table 3

Welding parameters

Bead	Amperage [A]	Current [V]	Welding speed [cm/min]	Heat input [KJ/cm]
1	220	21	24	8,08
2	220	21	25	7,8
3	220	22	25	8,1
4	220	22	22	9,2

The experimental stand to conduct the investigation is presented in figure 2. The geometric model was developed in the MSC APEX software program, and the simulation of the deposition process of the four beads was

performed by the Simufact Welding program. Both the equipment and the software employed to develop and validate the numerical model are part of the infrastructure of the Advanced Welding Research Center - SUDAV from "Dunarea de Jos" University of Galati, Faculty of Engineering, Department of Manufacturing Engineering.

Fig. 2. Stand for experimental measurements.

2.3. Finite Element Method

To simulate the deposition welding of the multicomponent alloy on the surface of the S235 steel plate, for all four weld beads, the heat source was considered to be a semi-ellipsoidal. The geometric model and the mesh with finite elements are presented in figure 3.

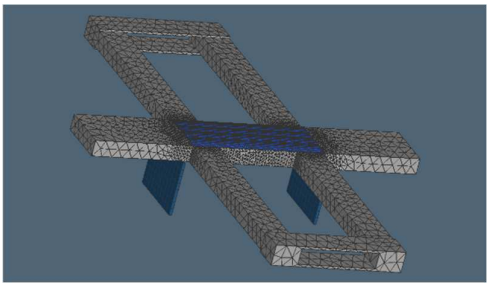

Fig. 3. Geometric model prepared for simulation.

To develop the element finite mesh, the tetrahedral type finite element was selected, as it is recommended in the literature for the thermostructural analysis. A special attention was given to the Heat Affected Zone (HAZ), whose mesh was refined because in this area, which is considered the most vulnerable region of the joint, significant thermo-mechanical modifications are developed [42–45]. The 3D model, developed by the authors, comprises 270278 nodes and 138612 elements for the steel plate and 9262 nodes and 5962 elements for the deposited weld beads. The heat flow is considered volumetric semi-ellipsoid, according to the heat source model developed by Goldak. The model of the heat source is shown in figure 4, where b is the width, d is depth, a_f is the length of the front, and a_r is the length of the rear, respectively. Based on the welding parameters, the dimensions, computed by the software, are presented in table 4.

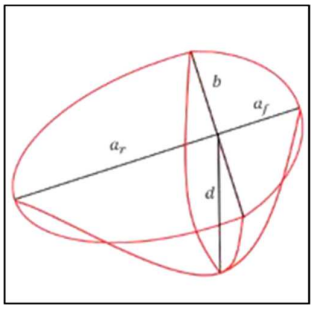

Fig. 4. Goldak model of heat source.

Table 4

Heat source dimensions

Bead	a_f [mm]	a_r[mm]	b[mm]	d[mm]
1	2.77	11.09	3.74	7.8
2	3.04	12.16	4.28	8.92
3	3.09	12.36	4.38	9.13
4	3.23	12.94	4.67	9.73

To validate the model, a comparative analysis of the numerical and experimental results has been made. Four strain gauges were used, placed in the points marked with a, b, c, and d, and six thermocouples, placed in points 1-6 (Fig. 5). Because several measurement errors occurred during the experiments, the values in 2 and 6 positions have not been recorded.

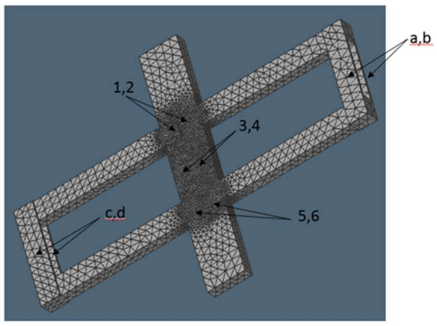

Fig. 5. Strain gouges and thermocouples placement.

3. RESULTS AND DISCUSSION

Figure 6 shows the thermal history recorded in the locations 1, 3, ,4 and 5, and the temperature profile correlated with the order of weld beads made by multi-deposition welding. The maximum temperature reaches 600-700°C on the second and third weld deposition, in accordance with the thermocouple position.

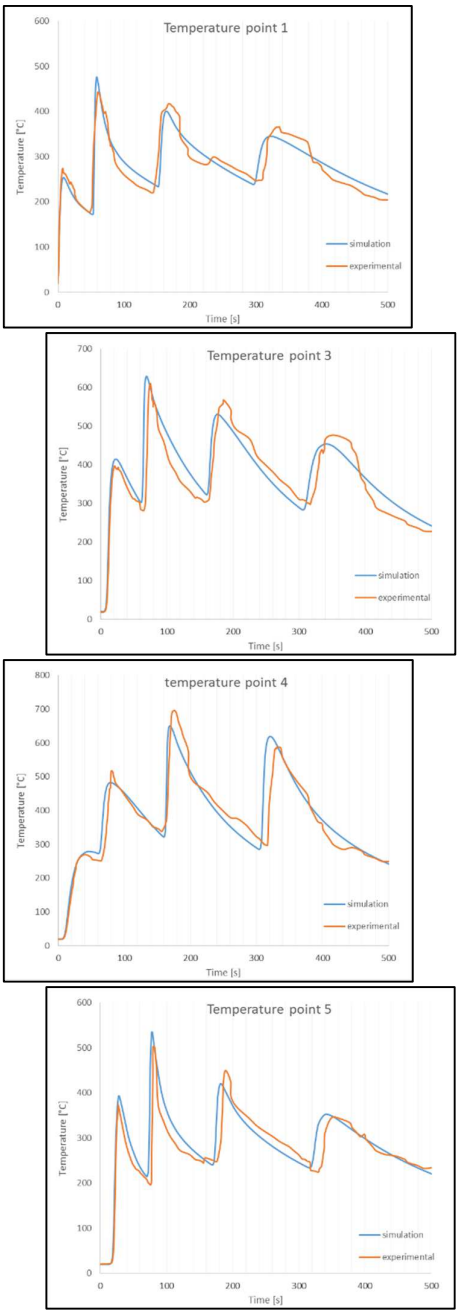

Fig. 6. Thermal cycles achieved by simulation and experimental test.

The normal stress profile achieved by Finite Element Modelling (FEM) and experiments is depicted in Figure 7. The strain gauges pairs (a-b and c-d) show the development of tensile stress on one side and the compression stress on the opposite side, the maximum value being 150-200MPa. The results suggest that the maximum displacement is developed perpendicularly to the deposition.

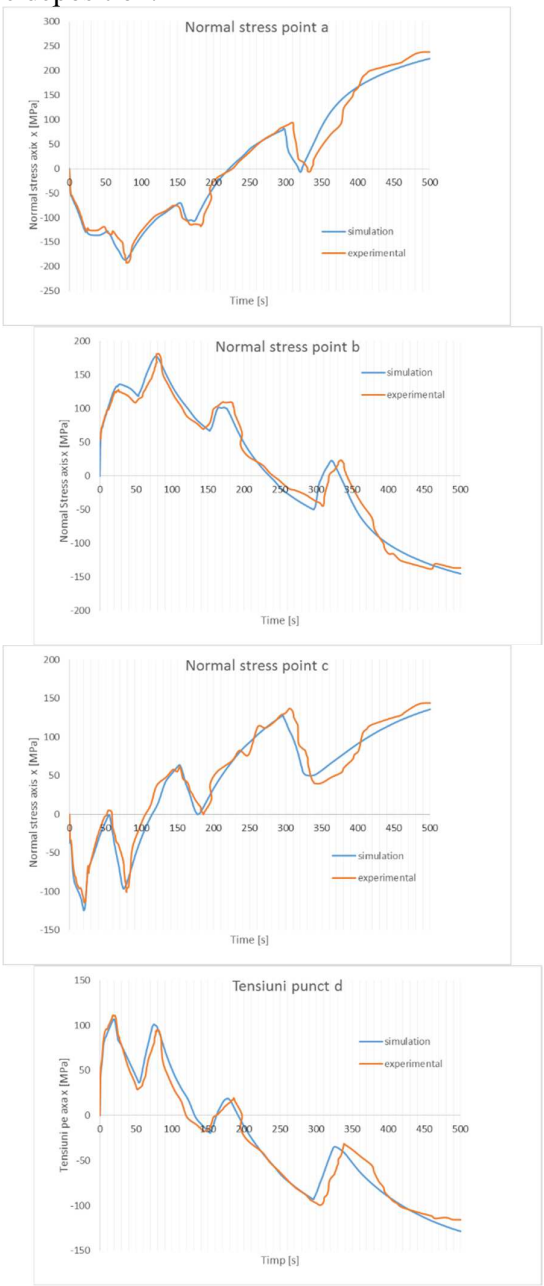

Fig. 7. Normal stress vs. time profile: numerical and experimental results.

Comparing the numerical and experimental results, the errors of 7-8% showed a good

agreement between the values measured and calculated [46,47].
The temperature field, generated during the deposition welding process, reveals a maximum temperature of 1700-1800°C in the molten metal pool, which is the usual peak temperature reported in scientific literature.

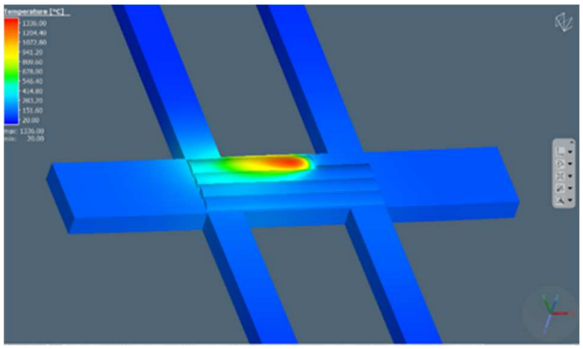

Fig. 8. Temperature field distribution.

The thermal analysis allows to estimate the depth of the HAZ for all deposited weld beads, revealing increased values from 5.3mm (first deposition) to 6.2mm, 6.3mm, and 6.6mm (the fourth deposition), as can be seen in figure 9. The reason why the lowest width of the HAZ in the steel substrate was measured at the first deposition is that the deposition of the multicomponent alloy was made without preheating. As the deposition process progressed, the base material heated up, and an increase in HAZ width was observed for the next depositions.

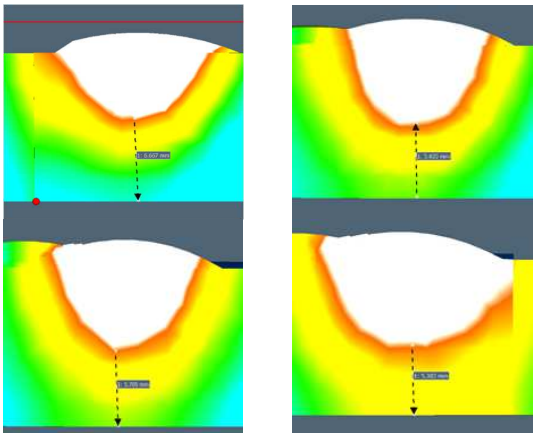

Fig. 9. HAZ depth predicted in the steel substrate.

The highest value, measured in the fourth deposition is significantly influenced by cumulation of thermal effects generated by the welding process in the previous depositions.
The distribution of the equivalent stress field, developed during the deposition of the last weld bead, is shown in figure 10. The maximum stress values reach 600-700MPa in the AlCr0.7FeNi multicomponent alloy (material having 1400-2100MPa tensile strength) and 300MPa in the S235 steel plate (steel having 440-450MPa tensile strength). In the deposited material, the stress is lowest near the molten metal pool and continuously increases during solidification. It is also found that the stress level decreases when a new bead is deposited, the effect being similar to a heat treatment effect generated by the welding deposition process.

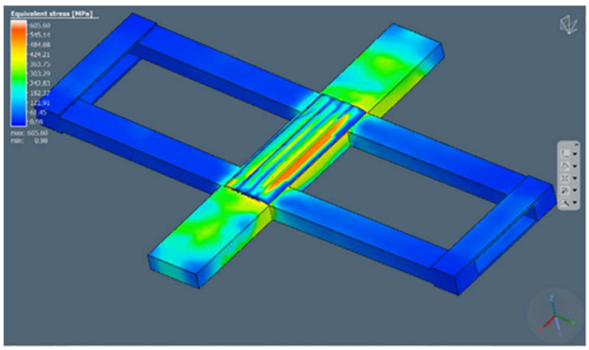

Fig. 10. Equivalent stress distribution.

5. CONCLUSIONS

Based on the experimental results and finite element analysis related to the behaviour of this new multicomponent material, the following conclusions can be summarized:

- The peak temperature reached in the molten metal pool is about 1700-1800°C, values that are similar to the results reported usually in scientific literature.
- The measured width of the Heat Affected Zone (HAZ) is 5.3-6.6mm and increases due to the thermal effects generated by the multi-deposition welding process.
- The peak equivalent stress reaches 600-700MPa in the multicomponent alloy deposited by welding and 300MPa in the S235 steel substrate.
- The numerical model developed for simulation of the $AlCr_{0.7}FeNi$ alloy deposition process on S235 steel substrate

material was validated by analysing comparatively the experimental and numerical values of temperature and stress fields. The errors computed are up to 7-8% that represents a good match between the results achieved by experiments and finite element modeling.

6. REFERENCES

[1] Miracle, D.B.; Senkov, O.N., *A Critical Review of High Entropy Alloys and Related Concepts*, Acta Mater. 2017, 122, 448–511, doi:10.1016/j.actamat.2016.08.081.

[2] George, E.P.; Curtin, W.A.; Tasan, C.C., *High Entropy Alloys: A Focused Review of Mechanical Properties and Deformation Mechanisms*, Acta Mater. 2020, 188, 435–474, doi:10.1016/j.actamat.2019.12.015.

[3] Sharma, P.; Dwivedi, V.K.; Dwivedi, S.P., *Development of High Entropy Alloys: A Review*, Mater. Today Proc. 2021, 43, 502–509, doi:10.1016/j.matpr.2020.12.023.

[4] Scutelnicu, E.; Simion, G.; Rusu, C.C.; Gheonea, M.C.; Voiculescu, I.; Geanta, V., *High Entropy Alloys Behaviour During Welding*, Rev. Chim. 2001, 71, 219–233, doi:10.37358/RC.20.3.7991.

[5] George, E.P.; Raabe, D.; Ritchie, R.O., *High-Entropy Alloys*, Nat. Rev. Mater. 2019, 4, 515–534, doi:10.1038/s41578-019-0121-4.

[6] Tsai M.-H., Yeh J.W., *High-Entropy Alloys: A Critical Review*, Materials Research Letters, 2014, Vol, 2, Nr. 3, 107-123

[7] Gali A., George E.P., *Tensile properties of high- and medium-entropy alloys*, Intermetallics, Vol. 39, 2013, pp. 74–78.

[8] Senkov O. N., Wilks G.B., Miracle D.B., Chuang C.P., Liaw P.K., *Refractory high-entropy alloys*, Intermetallics, Vol. 18, Issue 9, 2010, pp. 1758-1765.

[9] Voiculescu I., Geanta, V., Ionescu, M., *Effects of heat treatments on the microstructure and microhardness of AlxCrFeNiMn alloys*, Annals of "Dunarea de Jos" University of Galati, Fascicle XII, Welding Equipment and Technology, 26, 2015, pp. 5-11.

[10] Wu Z., Bei H., Pharr G.M., George E.P., *Temperature dependence of the mechanical properties of equiatomic solid solution alloys with face-centered cubic crystal structures*, Acta Materialia, Vol. 81, 2014, pp. 428-441.

[11] Senkov O. N., Wilks G. B., Scott J. M., Miracle D.B., *Mechanical properties of Nb25Mo25Ta25W25 and V20Nb20Mo20Ta20W20 refractory high entropy alloys*, Intermetallics, Vol. 19, Issue 5, 2011, pp. 698-706.

[12] Gludovatz B., Hohenwarter A., Catoor D., Chang E. H., George E. P., Ritchie R.O., *A fracture-resistant high-entropy alloy for cryogenic applications*, Science,Vol. 345, 2014, Issue 6201, pp. 1153-1158.

[13] He J. Y., Wang H., Huang H.L., Xu X. D., Chen M. W.,Wu Y., Liu X. J., Nieh T.G., *An K., Lu Z. P., A precipitation-hardened high-entropy alloy with outstanding tensile properties*, Acta Materialia, Vol. 102, 2016, pp. 187-196.

[14] Voiculescu I., Geanta V., Scutelnicu E., Stefanoiu R., Rotariu A., Solomon Gh., *Joining methods of high entropy alloys used for ballistic targets*, 1st World Conference on Advanced Materials for Defense, AuxDefense 2018, Lisbon, 2018.

[15] Lu Y. P., Gao X. Z., Jiang L., Chen Z. N., Wang T. M., Jie J. C., Kang H. J., Zhang Y. B., Guo S., Ruan H. H., Zhao Y. H., Cao Z. Q., Li T. J., *Directly cast bulk eutectic and neareutectic high entropy alloys with balanced strength and ductility in a wide temperature range*, Acta Materialia, Vol. 124, 2017, pp. 143-150.

[16] Tang Z., Yuan T., Tsai C. W., Yeh J. W., Lundin C. D., Liaw P. K., *Fatigue behavior of wrought Al0.5CoCrCuFeNi two-phase high-entropy alloy*, Acta Materialia, Vol. 99, 2015, pag. 247-258.

[17] Youssef K. M., Zaddach A. J., Niu C., Irving D. L., Koch C. C., A *Novel Low-Density, High-Hardness, High-entropy Alloy with Close-packed Single-phase Nanocrystalline Structures*, Materials Research Letters, Vol. 3, 2015, pp. 95-99.

[18] Zhu J. M., Fu H. M., Zhang H. F., Wang A. M., Li H., Hua Z.Q., *Microstructures and compressive properties of multicomponent AlCoCrFeNiMox alloys*, Materials Science and Engineering A, Vol. 527, 2010, pag. 6975-6979.

[19] Gorsse S., NguyenM. H., Senkov O. N., Miracle D. B., *Database on the mechanical properties of high entropy alloys and complex concentrated alloys*, Data in Brief, Vol. 21, 2018, pag. 2664-2678.

[20] Thi-Cam Nguyen N., Moon J., Sathiyamoorthi P., Asghari-Rad P., Kim G., Lee C.S., Kim H.S., *Superplasticity of V10Cr15Mn5Fe35Co10Ni25*

high-entropy alloy processed using high-pressure torsion, Materials Science and Engineering: A, 2019, Vol. 764, 9, 138198

[21] Liu J., Guo X., Lin Q., He Z., An X., Li L., Liaw P. K., Liao X., Yu L., Lin J., Xie L., Ren J., Zhang Y., *Excellent ductility and serration feature of metastable CoCrFeNi high-entropy alloy at extremely low temperatures*, SCIENCE CHINA Materials, 2018.

[22] Zherebtsov S., Stepanov N., Ivanisenko Y., Shaysultanov D., Yurchenko N., Klimova M., Salishchev G., *Evolution of Microstructure and Mechanical Properties of a CoCrFeMnNi High-Entropy Alloy during High-Pressure Torsion at Room and Cryogenic Temperatures*, Metals, 2018.

[23] Waseem O.A., Ryu H.J., *Combinatorial development of the low-density high-entropy alloy Al10Cr20Mo20Nb20Ti20Zr10 having gigapascal strength at 1000 °C*, Journal of Alloys and Compounds, Vol. 845, 2020.

[24] Wang W. R., Wang W. L., Yeh J. W., *Phases, microstructure and mechanical properties of AlxCoCrFeNi high-entropy alloys at elevated temperatures*, Journal of Alloys and Compounds, Vol. 589, 2014, 143-152.

[25] Li, J.; Huang, Y.; Meng, X.; Xie, Y. A *Review on High Entropy Alloys Coatings: Fabrication Processes and Property Assessment.* Adv. Eng. Mater. 2019, 21, 1900343, doi:10.1002/adem.201900343.

[26] Arif, Z.U.; Khalid, M.Y.; ur Rehman, E.; Ullah, S.; Atif, M.; Tariq, A. *A Review on Laser Cladding of High-Entropy Alloys, Their Recent Trends and Potential Applications*. J. Manuf. Process. 2021, 68, 225–273, doi:10.1016/j.jmapro.2021.06.041.

[27] Sharma, A.. *High Entropy Alloy Coatings and Technology*, Coatings 2021, 11, 372, doi:10.3390/coatings11040372.

[28] Meghwal, A.; Anupam, A.; Murty, B.S.; Berndt, C.C.; Kottada, R.S.; Ang, A.S.M., *Thermal Spray High-Entropy Alloy Coatings: A Review*., J. Therm. Spray Technol. 2020, 29, 857–893, doi:10.1007/s11666-020-01047-0

[29] Duchaniya, R.K.; Pandel, U.; Rao, P. *Coatings Based on High Entropy Alloys: An Overview*, Mater. Today Proc. 2021, 44, 4467–4473, doi:10.1016/j.matpr.2020.10.720.

[30] Liao, W.-B.; Zhang, H.; Liu, Z.-Y.; Li, P.-F.; Huang, J.-J.; Yu, C.-Y.; Lu, Y., *High Strength and Deformation Mechanisms of Al0.3CoCrFeNi High-Entropy Alloy Thin Films Fabricated by Magnetron Sputtering*. Entropy 2019, 21, 146, doi:10.3390/e21020146.

[31] Liao, W.; Lan, S.; Gao, L.; Zhang, H.; Xu, S.; Song, J.; Wang, X.; Lu, Y., *Nanocrystalline High-Entropy Alloy (CoCrFeNiAl0.3) Thin-Film Coating by Magnetron Sputtering*, Thin Solid Films 2017, 638, 383–388, doi:10.1016/j.tsf.2017.08.006.

[32] Jiang, Y.Q.; Li, J.; Juan, Y.F.; Lu, Z.J.; Jia, W.L., *Evolution in Microstructure and Corrosion Behavior of AlCoCrxFeNi High-Entropy Alloy Coatings Fabricated by Laser Cladding*, J. Alloys Compd. 2019, 775, 1–14, doi:10.1016/j.jallcom.2018.10.091.

[33] Liu, J.; Liu, H.; Chen, P.; Hao, J., *Microstructural Characterization and Corrosion Behaviour of AlCoCrFeNiTix High-Entropy Alloy Coatings Fabricated by Laser Cladding*, Surf. Coat. Technol. 2019, 361, 63–74, doi: 10.1016/j.surfcoat.2019.01.044.

[34] Fereidouni, M.; Sarkari Khorrami, M.; Heydarzadeh Sohi, M., *Liquid Phase Cladding of AlxCoCrFeNi High Entropy Alloys on AISI 304L Stainless Steel*, Surf. Coat. Technol. 2020, 402, 126331, doi:10.1016/j.surfcoat.2020.126331.

[35] Huo, W.; Shi, H.; Ren, X.; Zhang, J., *Microstructure and Wear Behavior of CoCrFeMnNbNi High-Entropy Alloy Coating by TIG Cladding*. Adv. Mater. Sci. Eng. 2015, 2015, 1–5, doi:10.1155/2015/647351.

[36] Shang, C.; Axinte, E.; Sun, J.; Li, X.; Li, P.; Du, J.; Qiao, P.; Wang, Y., *CoCrFeNi(W1−xMox) High-Entropy Alloy Coatings with Excellent Mechanical Properties and Corrosion Resistance Prepared by Mechanical Alloying and Hot Pressing Sintering*. Mater. Des. 2017, 117, 193–202, doi:10.1016/j.matdes.2016.12.076.

[37] Tang, Y.; Wang, S.; Sun, B.; Wang, Y.; Qiao, Y., *Fabrication and wear behavior analysis on AlCrFeNi high entropy alloy coating under dry sliding and oil lubrication test conditions*. Surf. Rev. Lett. 2016, 23, 1650018, doi:10.1142/S0218625X16500189.

[38] Ren M.; Wang G.; Li B., *Microstructure and properties of AlCrFeNi intermetallic for electronic packaging shell*, 18th International Conference on Electronic Packaging Technology

(ICEPT), 2017, doi: 10.1109/ICEPT.2017.8046570

[39]Dong Y;, Lu Y.; Kong J.; Zhang J.; Li T.; *Microstructure and mechanical properties of multi-component AlCrFeNiMox high-entropy alloys*, Journal of Alloys and Compounds, Vol. 573, 2013, pp. 96-101, doi: 10.1016/j.jallcom.2013.03.253

[40]Voiculescu, I.; Geanta, V.; Stefanescu, E.V.; Simion, G.; Scutelnicu, E., *Effect of Diffusion on Dissimilar Welded Joint between Al0.8CoCrFeNi High-Entropy Alloy and S235JR Structural Steel*, Metals **2022**, *12*, 548, doi:10.3390/met12040548

[41]Mitru, A.; Semenescu, A.; Simion, G.; Scutelnicu, E.; Voiculescu, I., *Study on the Weldability of Copper—304L Stainless Steel Dissimilar Joint Performed by Robotic Gas Tungsten Arc Welding*, Materials **2022**, *15*, 5535, doi:10.3390/ma15165535.

[42]Mocanu, C.I.; Tudose, D.I.; Hadar, A.; Gavan, E., *Strains and Stresses at Welding with Tubular Wires and Swinging the Electric Arc*. *IOP Conf. Ser.:* Mater. Sci. Eng. **2022**, *1262*, 012053, doi:10.1088/1757-899X/1262/1/012053.

[43]Birsan, D.C.; Simion, G.; Voiculescu, I.; Scutelnicu, E., *Numerical Model Developed for Thermo-Mecahnical Analysis in AlCrFeMnNiHf0.05–Armox 500 Steel Welded Joint,* AWET **2021**, *32*, 37–46, doi:10.35219/awet.2021.05.

[44]Birsan, D.C.; Simion, G., *Numerical Modelling of Thermo-Mechanical Effects Developed in Resistance Spot Welding of E304 Steel with Copper Interlayer*. AWET **2022**, *33*, 89–94, doi:10.35219/awet.2022.07.

[45]Birsan, D.; Scutelnicu, E.; Visan, D., *Behaviour Simulation of Aluminium Alloy 6082-T6 during Friction Stir Welding and Tungsten Inert Gas Welding*.; Barcelona, Spain, September 2011; pp. 103–108.

[46]Suman, S.; Biswas, P., *Microstructural, Strength and Residual Stress Studies on Single- and Double-Side Single-Pass Submerged Arc Welding of 9Cr–1Mo–V Steel Plate*, J. Inst. Eng. India Ser. C **2022**, *103*, 1177–1191, doi:10.1007/s40032-022-00870-4.

[47]Ahmad, A.S.; Wu, Y.; Gong, H.; Liu, L., *Numerical Simulation of Thermal and Residual Stress Field Induced by Three-Pass TIG Welding of Al 2219 Considering the Effect of Interpass Cooling*, Int. J. Precis. Eng. Manuf. **2020**, *21*, 1501–1518, doi:10.1007/s12541-020-00357-1.

SIMULAREA PRIN MEF A PROCESULUI DE DEPUNERE PRIN SUDARE WIG A UNUI ALIAJ MULTICOMPONENT PE SUBSTRAT DE OȚEL CARBON

Rezumat: Datorită costului ridicat de producție a aliajelor multicomponent, aplicabilitatea acestor materiale în industrie este încă limitată. Procesul de depunere prin sudare sau placarea ar trebui luat în consideraţie ca fiind o soluție mai puțin costisitoare şi mai accesibilă pentru obținerea acestor materiale speciale, materiale care pot fi folosite în multe aplicații industriale. Această lucrare prezintă un model numeric care simulează depunerea prin sudare a unui aliaj multicomponent, din sistemul AlCrFeNi, pe un substrat de oțel structural S235. Modelul a fost validat experimental prin măsurarea temperaturii și a nivelului de tensiuni dezvoltat în timpul procesului de depunere a patru cordoane de sudură. Rezultatele numerice au evidențiat valori maxime ale temperaturii de 1700-1800°C în baia de metal topit și un nivel maxim al tensiunilor echivalente de 600-700MPa în materialul multicomponent depus prin sudare.

George SIMION, PhD Student, ”Dunarea de Jos” University of Galati, Faculty of Engineering, Department of Manufacturing Engineering, Romania, george.simion@ugal.ro, +40336130208

Dan BÎRSAN, Asist. Prof. PhD, ”Dunarea de Jos” University of Galati, Faculty of Engineering, Department of Manufacturing Engineering, Romania, dan.birsan@ugal.ro, +40336130208

Ionelia VOICULESCU, Professor, Politehnica University of Bucharest, Faculty of Industrial Engineering and Robotics, Department of Quality Engineering and Industrial Technologies, Romania, ioneliav@yahoo.co.uk, +40214029302

Elena SCUTELNICU, Professor, ”Dunarea de Jos” University of Galati, Faculty of Engineering, Department of Manufacturing Engineering, Romania, elena.scutelnicu@ugal.ro, +40336130208